

Local Magnetic Investigations of MgB₂ Bulk Samples for Magnetic Shielding Applications

Laura Gozzelino, Bruno Minetti, Roberto Gerbaldo, Gianluca Ghigo, Francesco Laviano, Angelo Agostino and Enrica Mezzetti

Abstract— A local magnetic characterization of disk-shaped MgB₂ bulk samples synthesized by the Spark-Plasma-Sintering technique was carried out aimed at studying the material magnetic shielding properties. This growth technique allows one to produce samples in different shapes and sizes as required for shielding applications. The analysis employed a linear array of Hall probes mounted on a custom-designed stage able to move perpendicular to the sample surface with micrometric resolution. Spatial distributions of the axial component of the shielding magnetic-induction field generated by the superconductor were evaluated in the temperature range 20-36 K and in applied magnetic field up to 1.5 T. By the analysis of these shielding field profiles in the framework of the critical state model, critical current densities, J_c , higher than 10^{10} A/m² were found at $T = 20$ K. On the basis of the found J_c values a preliminary estimation of the full penetration field inside a tube-shaped shield component was carried out. It indicates that the material under test is a good candidate for passive magnetic shields.

Index Terms—Local magnetic analysis, Magnetic shielding, MgB₂, Critical current density

I. INTRODUCTION

MAGNETIC field shielding has a twofold purpose. It is indeed required in order to reduce the magnetic field produced by a device, protecting the neighboring equipments and the personnel operating very near to it (see for example magneto-resonance imaging equipment in medical sector [1],[2]). On the other side, magnetic shielding allows the correct operation of sensitive detectors (see for example equipments for magneto-cardiography and magneto-encephalography [3]) protecting them from the electromagnetic noise emitted in the surroundings.

In this framework of passive shielding, bulk superconductors play an important role due to their ability to expel magnetic fields. For the last years this solution has become very attractive due to the cost reduction guaranteed by the use of high temperature cuprate superconductors (HTSC) [4]-[12]. However HTSC brittleness problems can make difficult and expensive the system scalability.

Manuscript received 3 August 2010. This work was supported by MIUR under PRIN project No.2007AW2K4Y.

L. Gozzelino, B. Minetti, R. Gerbaldo, G. Ghigo, F. Laviano and E. Mezzetti are with Dept. of Physics, Politecnico di Torino, Torino, Italy (corresponding author: Bruno Minetti, phone: +39-011-5647317; fax: +39-011-5647399; e-mail: bruno.minetti@polito.it).

A. Agostino is with Dept. of General and Organic Chemistry, Università di Torino, Torino, Italy.

The superconducting compound MgB₂ allows overcoming both refrigeration and manufacturing costs. The operating temperature (20-30 K) is indeed easily reachable by means of single- or double-stages cryogen-free cryocooler. This allows a MgB₂-based shield installation in any location provided that an electrical supply is available. Besides this, MgB₂ base material and manufacturing costs are very low. MgB₂ can be used also in the polycrystalline state (showing a small barrier to the current flow at the grain boundaries due to its high coherence length [13]), and presents a lower density and a higher mechanical strength than HTSC.

Magnetic shielding properties of MgB₂ were already successfully checked [14]: noticeably MgB₂ tube was reported to be able to shield magnetic fields of 0.85 T at 13.3 K [15] opening an interesting applicative window.

In this paper we report on the analysis of the shielding magnetic-induction field of disk-shaped MgB₂ bulk samples synthesized by the SPS (Spark-Plasma-Sintering) technique [16]. Experimental spatial distributions of the axial component of the shielding field generated by the superconductor were measured in the temperature range 20-36 K and in applied magnetic field up to 1.5 T by means of an array of GaAs Hall probes aligned along a sample diameter. During measurements, the probe array was moved with micrometric resolution perpendicularly to the sample surface. Data were then analysed in the framework of the critical state model [17],[18] and the critical current density, J_c , is evaluated. Finally a rough estimation of the magnetic shielding capability of the material under study is outlined.

The paper is organized as follows. In Section II experimental details concerning MgB₂ growth technique and the custom-designed experimental setup used for the characterization are briefly described. Experimental results and discussion are reported in Section III. Finally, conclusions are summarized in Section IV.

II. EXPERIMENTAL DETAILS

MgB₂ samples were sintered into thin cylinder (disk) shape by the Spark-Plasma-Sintering technique using FCT – HP D 5 (FCT System GmbH, Germany) equipment. Such technique allows obtaining the compound in different sizes and shapes, as required for shield component manufacturing. Details on the growth process are reported elsewhere [19].

In this paper we deal with the characterization of a representative disk-shaped sample with a diameter of 20.30

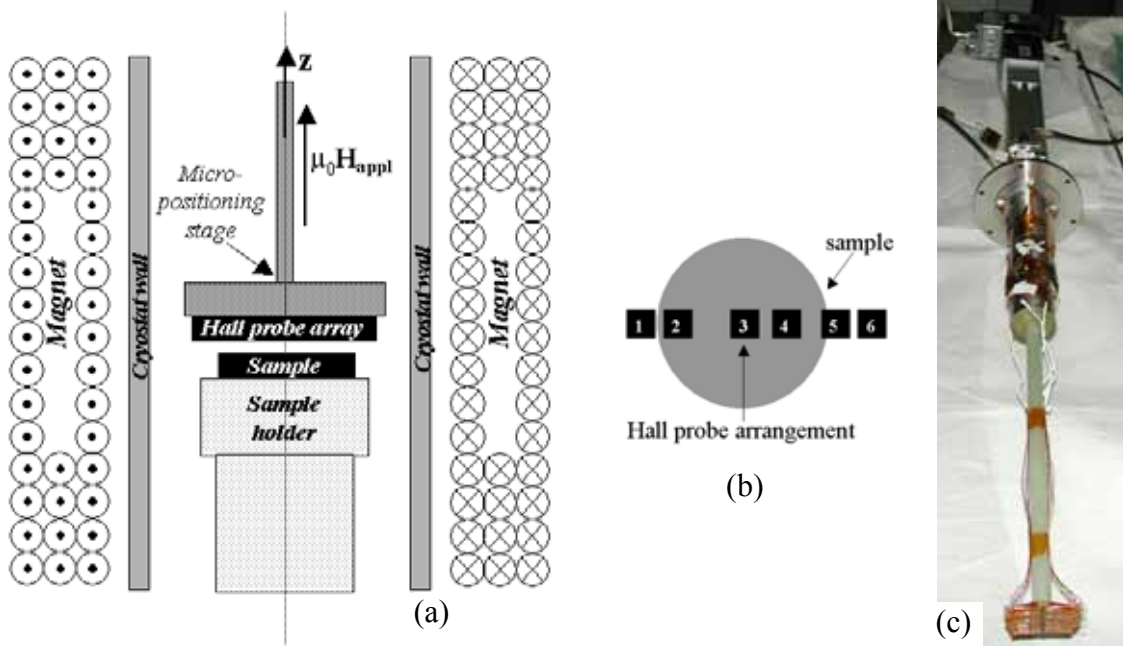


Fig. 1. (a) Experimental setup (not to scale): the linear array of Hall probes is mounted on the bottom surface of a motor-driven micro-positioning stage moving along the z -axis (axial direction). The sample is placed on the top surface of the second stage of the cryogen-free cryostat, at the center of the magnet coil. (b) Scheme of the Hall probe configuration related to the sample. (c) Custom designed cryogenic insert used for the magnetic characterization, equipped by the micro-positioning stage where the GaAs Hall probe array is mounted.

mm and a height of 3.44 mm. The sample was sintered at 1150°C , using a ramp rate of $160^{\circ}\text{C min}^{-1}$ and a holding time of 3 min at the maximum temperature. X-ray diffraction (XRD) on 10 - 100° 2θ scanned angle (Bragg-Brentano configuration with $\text{Cu K}\alpha$ radiation source) showed that the main phase is MgB_2 with a small amount of unreacted magnesium. The lattice parameters, determined by Rietveld refinement, are $a = 3.0861(1)$ and $c = 3.5247(6)$. Sample transition temperature is $T_c = 37.10$ K (defined as the inflection point in the resistive transition) whereas its transition width between the 10% and 90% values of the resistance drop is $\Delta T_c \sim 0.5$ K.

Magnetic characterizations were performed in a Leybold RNK 10-300 double-stage cryogen-free cryocooler using a custom-designed insert. The insert is equipped by a motor-driven micro-positioning stage with a linear travel range of 100 mm and a spatial resolution of $1\ \mu\text{m}$. The magnetic field was produced by a 6 T Cryomagnetics cryogen-free magnet.

The sample was placed on a temperature controlled sample holder at the top of the second cooling stage of the cryocooler in such a way that its center coincided with the magnet center. The magnetic field was applied perpendicular to the sample surface (see scheme in Fig. 1(a)).

The 3D distributions of the axial component (z -component) of the magnetic induction field, B_z , were carried out by moving along the axial direction (z -direction) an array of 6 GaAs Hall probes. Each probe has a disk-shaped active area with diameter of $300\ \mu\text{m}$ and a sensitivity of $41.5\ \text{mV/T}$ for a nominal current of $0.1\ \text{mA}$. The probes were aligned across a sample diameter on a 30 mm long line (see scheme in Fig. 1(b)) and fixed to the micro-positioning stage (Fig. 1(c)). The minimum gap between the sensing Hall probe elements and the sample surface was 1.6 mm.

The Hall probe voltage was measured by a 2182A Keithley

nanovoltmeter coupled to an 8-channel Keithley 7001 scanner. The applied magnetic field as well as the sample holder position and the Hall probe voltage acquisition system were controlled by a LabviewTM interface.

III. EXPERIMENTAL RESULTS AND DISCUSSION

Magnetic induction fields, B_z , were measured at different temperatures in the range 20-36 K under zero field cooling conditions. At each temperature the external field, $\mu_0 H_{\text{appl}}$, was stepped from 0 to 1.5 T and for each step, the B_z distribution was evaluated by moving the Hall probe array along the axial direction. The axial component of the shielding magnetic-induction field generated by the superconductor, B_{sz} , was then taken as difference between B_z and $\mu_0 H_{\text{appl}}$.

Figure 2 displays the $B_{sz}(z)$ profiles evaluated in the external field $\mu_0 H_{\text{appl}} = 1.0$ T at increasing temperatures ($T = 20$ K, 25 K and 30 K). The zero position of the Hall sensors along the axial direction was chosen coincident with the center of the sample. As expected, the shielding effect is maximum in correspondence to the sample center (Hall probe no. 3) and decreases towards the edges. The positive values of B_{sz} detected by the Hall probes no. 1, 5, 6 are due to the demagnetization effects at the disk edges [17],[18].

In order to extract the critical current density (J_c) values from the $B_{sz}(z)$ curves we applied the critical state model suggested in [17],[18] for modelling the flux penetration in a disk in transverse geometry. The disk was divided into an array of coaxial current loops centered on the z -axis, of increasing diameter ρ with $0 < \rho < R$ and vertical position z with $-d/2 < z < d/2$. Here R and d are the disk radius and thickness, respectively. The current $I(\rho, z)$ flowing in the i th loop is determined by $I(\rho, z) = J(\rho, z) d\rho dz$ where $J(\rho, z)$ is the current density at the position (ρ, z) of the loop. The axial

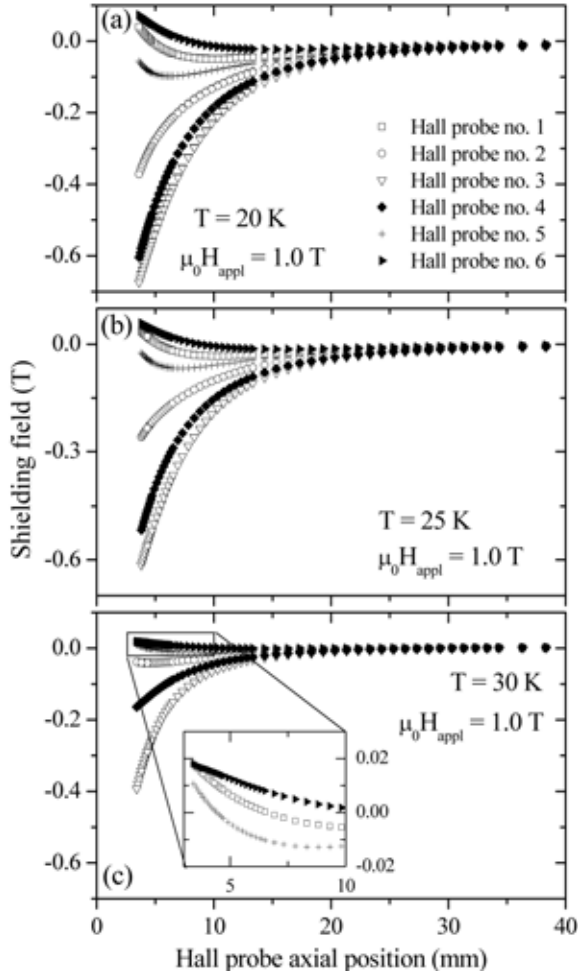


Fig. 2. Profiles of the axial component of the shielding magnetic-induction field, B_{sz} , at $T = 20$ K (a), 25 K (b) and 30 K (c). In all cases the external applied field was $\mu_0 H_{\text{appl}} = 1.0$ T. The axial position of the Hall sensors is measured starting from the center of the superconducting disk.

shielding field produced by the whole disk is then calculated by means of the Biot-Savart law. Its value, at the arbitrary coordinates ρ_0 and z_0 and for increasing external fields after zero field cooling, is given by [20]:

$$B_{sz}(\rho_0, z_0) = \frac{\mu_0}{2\pi} \int_{-\frac{d}{2}}^{\frac{d}{2}} dz \int_0^R G_z(\rho, z, \rho_0, z_0) J(\rho, z) d\rho \quad (1)$$

where

$$G_z(\rho, z, \rho_0, z_0) = \frac{\mu_0}{2\pi} \frac{1}{\left[(\rho + \rho_0)^2 + (z_0 - z)^2 \right]^{3/2}} \cdot \left[K(k^2) + \frac{\rho^2 - \rho_0^2 - (z_0 - z)^2}{(\rho_0 - \rho)^2 + (z_0 - z)^2} E(k^2) \right],$$

$K(k^2)$ and $E(k^2)$ are complete elliptic integrals of the first and second kind and $k^2 = \frac{4\rho_0\rho_i}{(\rho_0 + \rho_i)^2 + (z_0 - z_i)^2}$. Finally, by assuming that J_c is isotropic and does not depend on the axial z coordinate and on the local magnetic field inside the sample,

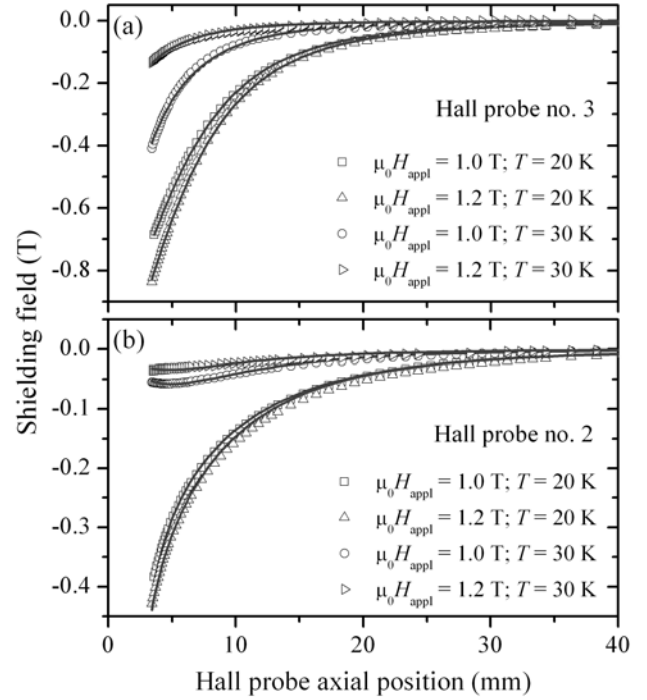


Fig. 3. Experimental $B_{sz}(z)$ curves (symbols) measured by means of the Hall probe no. 3 (a) and no. 2 (b) and corresponding fitting curves with (1) (solid lines).

the current density $J(r, z)$ is written as [17]:

$$J(\rho) = \begin{cases} -\left(\frac{2J_c}{\pi}\right) \arctan\left[\left(\frac{\rho}{R}\right) \sqrt{\frac{R^2 - a^2}{a^2 - \rho^2}}\right] & \rho \leq a \\ -J_c & a < \rho \leq R \end{cases}$$

where $a = R/\cosh(\mu_0 H_{\text{appl}}/B_d)$ is the inner radius of the annular vortex filled region and $B_d = \mu_0 J_c d/2$ is a characteristic field for disk geometry.

Figs. 3(a) and (b) show $B_{sz}(z)$ profiles measured by Hall probes no. 3 (located in the middle of the sample) and no. 2 (located near the edge of the sample), respectively, and the corresponding fitting curves with (1). The experimental profiles were obtained by applying the magnetic fields $\mu_0 H_{\text{appl}} = 1.0$ and 1.2 T at the temperatures $T = 20$ and 30 K. The theoretical fits, where J_c is the only free parameter, agree well with the experimental data. J_c values obtained by applying this fitting procedure to the $B_{sz}(z)$ profiles measured by Hall probe no. 3 at several temperatures and external applied fields are reported in Fig. 4. These values are in good agreement with those reported in literature for MgB_2 bulk samples [21],[22]. A similar J_c dependence on the applied magnetic field was observed by analyzing B_{sz} profiles measured by means of the other Hall probes. This points to a quite homogeneous pinning mechanism inside the sample.

Starting from the J_c values reported in Fig. 4, and following the model of field penetration into a superconducting tube suggested in [10], it is possible to roughly estimate the magnetic shielding properties of the material under study. By assuming that the critical current density is constant inside the superconductor and that its value only depends on the external

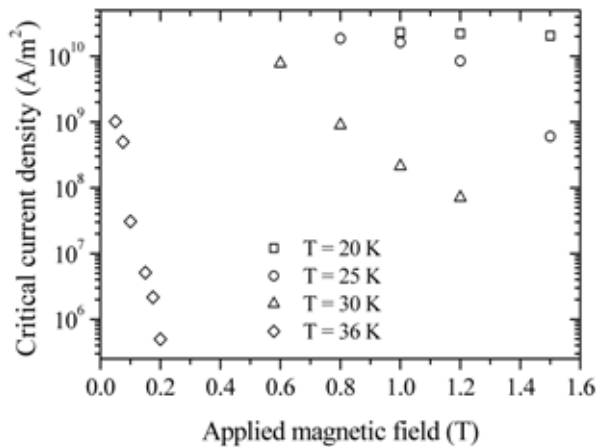


Fig. 4. Critical current density values as a function of the external applied field and for different temperatures. J_c values were obtained by fitting with (1) the $B_{z_2}(z)$ profiles measured by the Hall probe no. 3.

applied field, the full penetration field in the tube centre region, $\mu_0 H_p$, can be written as [10]:

$$\mu_0 H_p = \mu_0 J_c t \frac{l}{4a} \ln \left\{ \frac{4a}{l} + \left[1 + \left(\frac{4a}{l} \right)^2 \right]^{0.5} \right\}$$

where l is the tube length, t its wall thickness and a its average radius. Then we define B_{lim} as the maximum applied magnetic-induction field that can be attenuated more than one thousand times by the superconductor. It means $B_{lim}/B_{in} \geq 1000$, where B_{in} is the magnetic-induction field measured in the tube center. When $l \geq 6a$, the value of B_{lim} is very close to $\mu_0 H_p$ [10]. Therefore for a tube where $l = 10$ cm, $a = 1.5$ cm, $t = 0.1$ cm, taking into account the J_c dependence on the external applied field reported in Fig. 4, we obtain $B_{lim} = 1.43$ T at $T = 25$ K, $B_{lim} = 0.87$ T at $T = 30$ K and $B_{lim} = 0.098$ T at $T = 36$ K. Even if these B_{lim} values are overestimated due to the disregarded J_c dependence on local magnetic field inside the sample [10],[23], they indicate that our growth technique allows producing bulk materials which are good candidates for magnetic shields.

IV. CONCLUSIONS

A preliminary characterisation of the magnetic shielding properties of MgB_2 bulk samples synthesized by SPS technique were performed at temperatures ranging from 20 to 36 K and in applied magnetic fields up to 1.5 T.

The axial component of the shielding field generated by a disk-shaped shield-component was measured at different locations across the sample and at several distances from its surface. Measurements were performed by means of a linear Hall probe array suitably mounted on a custom-designed cryogenic insert moving perpendicular to the sample surface. Sample exhibits critical current density values higher than 10^{10} A/m² at $T = 20$ K and $\mu_0 H_{appl} = 1$ T, as evaluated by fitting the shielding field *versus* Hall probe-sample distance curves in the framework of the critical state model. A preliminary calculation of the shielding capability inside tube-shaped samples, carried out on the basis of the found J_c values,

indicates that the material under test is a good candidate for passive magnetic shields.

Further shielding tests on samples with different geometries and with superconducting joints are currently in progress.

REFERENCES

- [1] J G M Kok *et al.*, "Installation of the 1.5 T MRI accelerator next to clinical accelerators: impact of the fringe field," *Phys. Med. Biol.*, vol. 54, pp. 409-415, Aug. 2009.
- [2] T. Johnston, R Moser, K. Moeller, and T. M. Moriarty, "Intraoperative MRI: Safety," *Neurosurgery Clinics of North America*, vol. 20, pp. 147-153, Apr. 2009.
- [3] R. L. Fagaly, "Superconducting quantum interference devices instruments and applications," *Rev. Sci. Instrum.*, vol. 77, p. 101101, Oct. 2006
- [4] E. Tjukanov *et al.*, "Current persistence and magnetic shielding properties of $Y_1Ba_2Cu_3O_x$ tubes," *Phys. Rev. B*, vol. 36, pp. 7244-7247, Nov. 1987.
- [5] O. G. Symko, W. J. Yeh, D. J. Zheng, and S. Kulkarni "Magnetic shielding and relaxation characteristics of superconducting $YBa_2Cu_3O_7$ tubes," *J. Appl. Phys.*, vol. 65, pp. 2142-2144, Mar. 1989.
- [6] J. O. Willis, M. E. McHenry, M. P. Maley, and H. Sheinberg "Magnetic shielding by superconducting Y-Ba-Cu-O hollow cylinders," *IEEE Trans. Magn.*, vol. 25, pp. 2502-2505, Mar. 1989.
- [7] J. W. Purpura and T. R. Clem, "The fabrication and characterization of high temperature superconducting magnetic shields," *IEEE Trans Magn.*, vol. 25, pp. 2506-2510, Mar. 1989.
- [8] V. Plecháček *et al.*, "Magnetic Shielding and Trapping Properties of BPSCCO Superconducting Tubes", *IEEE Trans. Appl. Supercond.* vol. 5, pp. 528-531, Jun. 1995.
- [9] A. Omura, K. Kotani, K. Yasu, M. Itoh, "Analysis of the magnetic distribution within a high-temperature superconductor magnetic shielding cylinder by use of the finite element method", *J Phys. Chem. Solids*, vol. 67, pp. 43-46, Jan.-Mar. 2006.
- [10] S. Denis *et al.*, "Magnetic shielding properties of high-temperature superconducting tubes subjected to axial fields", *Supercond. Sci. Technol.*, vol. 20, pp. 192-201, Jan. 2007.
- [11] J-F. Fagnard, M. Dirickx, M. Ausloos, G. Lousberg, B. Vanderheyden, and Ph. Vanderbemden, "Magnetic shielding properties of high-Tc superconducting hollow cylinders: model combining experimental data for axial and transverse magnetic field configurations," *Supercond. Sci. Technol.*, vol. 22, p. 105002, Aug. 2009.
- [12] J-F. Fagnard *et al.*, "DC and AC Shielding Properties of Bulk High-Tc Superconducting Tubes," *IEEE Trans. Appl. Supercond.*, vol. 19, pp. 2905-2908, Jun. 2009.
- [13] X.X. Xi, "Two-band superconductor magnesium diboride," *Rep. Prog. Phys.*, vol. 71, p. 116501, Nov. 2008.
- [14] T. Cavallin, R. Quarantiello, A. Matrone, and G. Giunchi, "Magnetic shielding of MgB_2 tubes in applied DC and AC field," *J. Phys. Conf. Series*, vol. 43, pp. 1015-1018, 2006.
- [15] E. Perini *et al.*, "The magnetic characterization of a MgB_2 superconducting hollow cylinder, at variable temperatures up to T_c ," *IEEE Trans. Appl. Supercond.*, vol. 17, pp. 2730-2733, Jun. 2007.
- [16] M. Omori, "Sintering, consolidation, reaction and crystal growth by the spark plasma system (SPS)," *Mater. Sci Eng. A*, vol. 287, pp. 183-188, Aug. 2008.
- [17] J. R. Clem and A. Sanchez, "Hysteresis ac losses and susceptibility of thin superconducting disks," *Phys. Rev. B*, vol. 50, pp. 9355-9362, Oct. 1994.
- [18] E. H. Brandt, "Superconductor disks and cylinders in an axial magnetic field. I. Flux penetration and magnetization curves," *Phys. Rev. B*, vol. 58, pp. 6506-6522, Sep. 1998.
- [19] L. Gozzelino *et al.*, "Magnetic characterization of MgB_2 bulk superconductor for magnetic field mitigation solutions", *J Supercond. Novel Magn.*, to be published.
- [20] W. R. Smythe, *Static and Dynamic Electricity*, McGraw-Hill, New York, 1950.
- [21] M. Eisterer, "Magnetic properties and critical currents of MgB_2 ," *Supercond. Sci. Technol.*, vol. 20, pp. R47-R73, Oct. 2007.
- [22] T. A. Prikhna, "Properties of MgB_2 bulk," arXiv:0912.4906, Dec. 2009.
- [23] H. Nicolescu, R. Schmidmeier, B. Topolski, and P. J. Gielisse "Shielding effects in ceramic superconductors," *Physica C*, vol. 229, pp. 105-112, Aug. 1994.